A Numerical Simulation Method of Toner Transfer Considering Voltage Distribution of Transfer Belt

Shinji AOKI, Masaki SUKESAKO and Masami KADONAGA
Imaging Engine Development Division, Ricoh Company, Ltd.

Abstract

A simulation method using 2-D and 3-D models is proposed for analysis of primary transfer processes. In the method, the motion of toner particles between an organic photoconductor (OPC) and an intermediate transfer belt (ITB) is calculated with a 3-D parallel plate model, while the 2-D electric potential distribution of the ITB is used as a boundary condition. The electric potential distribution of the ITB is obtained by 2-D electric field calculation, where a vicinity of a transfer nip is modeled with a boundary-fitted coordinate system, and the Poisson equation is solved in consideration of the transfer bias, transfer member configurations, the Paschen discharge, electrical conduction and advection of electric charge. In the 3-D calculation, a space between the OPC and the ITB in a limited part of an image area is modeled in a 3-D parallel plate model, and the motion of toner particles, which obeys Newton's second law of motion, and the Poisson equation are solved in consideration of the electric potential of the belt, charge and adhesion of toner, the latent image on the OPC, and the Paschen discharge. The 3-D calculation is carried out with changing the transfer gap, while the electric potential of the ITB obtained by the 2-D calculation is applied to the lower surface of the ITB layer. The simulation method enables analysis of transfer processes with a low computational load, and simulated results of transfer efficiency and toner scattering show good agreement with experiments.

Introduction

Intermediate transfer systems have been widely used in electrophotographic printers. In the systems, a toner image developed on a photoconductor is primarily transferred onto an intermediate transfer member and is then secondarily transferred onto a sheet of paper. Since toner images are transferred by the electrostatic force, design of their electric field distribution is a key point for faithful transfer. Recently numerical methods have been applied to analysis of the electric field [1-5].

In numerical analysis of transfer processes, a smaller size of calculation grids than the diameter of toner particles is suitable for prediction of the transferred toner images, since the strength and the direction of the electrostatic force on individual toner particles, which determine the image quality, can be precisely evaluated. On the other hand, if the vicinity of a transfer nip is modeled using such a small size of calculation grids, the number of calculation grids becomes large and a considerable computational load is required, especially in 3-D analysis.

In the present work, a simulation method of a transfer process, which can predict the image quality with a low computational load, is proposed and analyses of a primary transfer process with an intermediate transfer belt are demonstrated.

Simulation Procedure and Model

In the simulation method, the motion of toner particles between an organic photoconductor (OPC) and an intermediate transfer belt (ITB) is calculated with a 3-D parallel plate model, while the electric potential of the ITB obtained by a 2-D electric field simulation is applied to a boundary condition. The simulation procedure is shown in Figure 1.

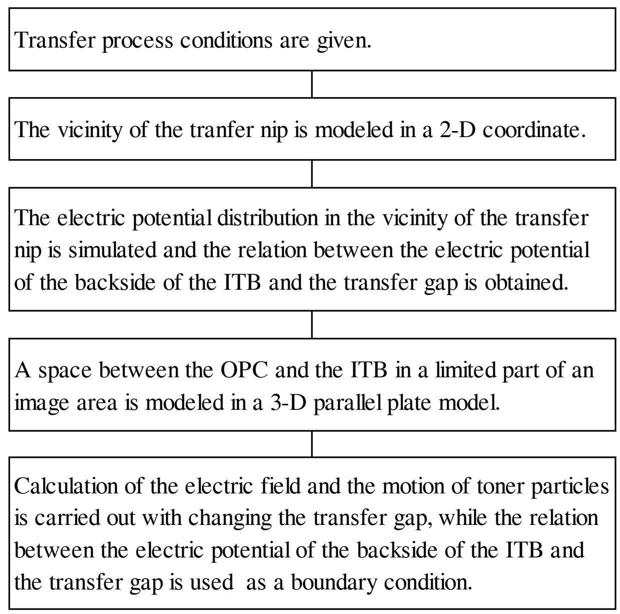

Figure 1. *Simulation procedure.*

A vicinity of a transfer nip in a printer is primarily modeled in a 2-D boundary-fitted coordinate system, where the size of calculation grids is set to be larger than the diameter of toner particles, and then the electric potential distribution is calculated including transfer bias, electrical characteristics of transfer members, transport of electric charges, and electrostatic discharge. The OPC, which has a latent image, and developed toner are dealt with as uniform layers at the initial state. An example of the 2-D model is shown in Figure 2.

The electric field $\mathbf{E}$ and the electric potential ϕ in the analysis area are solved with the Poisson equation:

$$\mathrm{div}\ \mathbf{E} = -\mathrm{div}\ (\mathrm{grad}\ \phi) = \rho / \varepsilon \qquad (1),$$

where ρ is the electric charge density and ε is the permittivity.

The electric charge density ρ is obtained by considering transport of electric charges and electrostatic discharge. The transport of the electric charges is expressed by the equation of continuity:

$$\partial\rho / \partial t = -\mathrm{div}\, \mathbf{J} \quad (2),$$

where t is the time and **J** is the current density.

The current density **J** is calculated including the electrical conduction and the advection as follows:

$$\mathbf{J} = \sigma\mathbf{E} + \rho\mathbf{v}_p \quad (3),$$

where σ is the electrical conductivity and $\mathbf{v}_p$ is the process velocity of the printer.

On condition that the ITB is made of such a carbon-filled plastic, the electric field dependence of the electrical conductivity σ is considered. In the present model, the field dependence of the electrical conductivity σ is reflected by using the Poole-Frenkel law [6]:

$$\sigma = \alpha \exp(\beta|\mathbf{E}|^{1/2}) \quad (4),$$

where α and β are empirical constants determined by a resistivity measurement.

The effect of electrostatic discharge is considered by adding electric charges on object surfaces forming an air gap, when the electric potential difference across the air gap exceeds the Paschen limit. The relations between the Paschen limit ϕ_{pa}, in units of volts, and the air gap G, in units of meters, are as follows [7]:

$$\phi_{pa} = \begin{cases} 75.4 \times 10^{6} \times G & (G < 4.8 \times 10^{-6}) \\ 362 & (8 \times 10^{-6} \geq G \geq 4.8 \times 10^{-6}) \\ 312 + 6.2 \times 10^{6} \times G & (G > 8 \times 10^{-6}) \end{cases} \quad (5).$$

The amount of electrostatic discharge Q, in units of coulomb per square meter, is estimated by the following equation:

$$Q = \varepsilon_o\, (\Delta\phi - \phi_{pa})\, (\Sigma(d_i / \varepsilon_i) + G) / (G\Sigma(d_i / \varepsilon_i)) \quad (6),$$

where $\Delta\phi$ is the electric potential difference across the air gap in units of volts, ε_o is the vacuum permittivity, and ε_i and d_i are the relative dielectric constant and the thickness of objects, respectively.

The above equations are solved until a steady state ($\partial\mathbf{E} / \partial t = 0$) is reached and the relation between the electric potential of the backside of the ITB and the transfer gap is obtained.

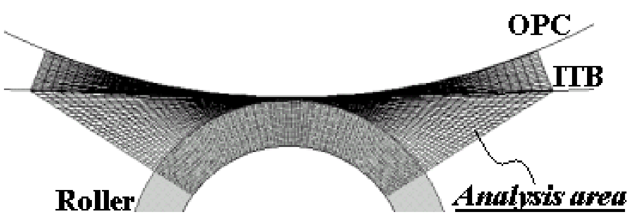

Figure 2. A schematic illustration of the 2-D model.

In the next step, a space between a part of the toner image on the OPC and the ITB is modeled in a 3-D parallel plate model with the smaller size of calculation grids than the diameter of toner particles. And then calculation of the electric field and the motion of toner particles is carried out with changing the transfer gap, while the relation between the electric potential of the backside of the ITB and the transfer gap is used as a boundary condition.

At the initial state, the latent image and toner particles exist on the surface of the OPC, and toner particles are adhering to the OPC due to electrostatic and non-electrostatic force. An example of the 3-D model is shown in Figure 3.

The electric field **E** and the electric potential ϕ in the analysis area are solved again by the Poisson equation (Eq. 1) with considering the Paschen discharge (Eq. 5 and 6). The electrostatic force acting on a toner particle $\mathbf{F}_e$ is related to the quantity of electric charge of the toner particle q and the electric field **E** as the following Equation (7):

$$\mathbf{F}_e = q\mathbf{E} \quad (7),$$

and the motion of the toner particle is calculated by Newton's second law of motion:

$$\mathbf{F}_e = d\,(m_t\mathbf{v}_t) / dt \quad (8),$$

where m_t and $\mathbf{v}_t$ are the mass and the velocity of the toner particle, respectively.

In the present model, the toner particle begins to move when the electrostatic force acting on the toner particle $\mathbf{F}_e$ overcomes the non-electrostatic adhesion force, and continues to move until it reaches the surface of the ITB. Collisions between toner particles are not considered.

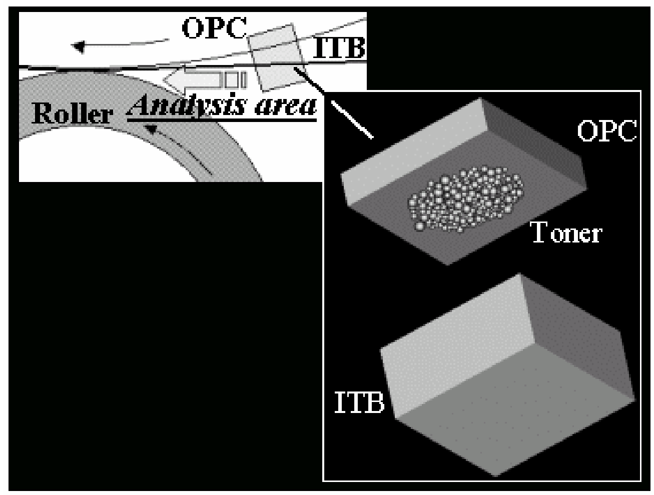

Figure 3. A schematic illustration of the 3-D model.

Experimental Validation of the 2-D and the 3-D Models

Before analyzing transfer processes in printers, validation experiments of the 2-D and the 3-D models have been separately carried out.

The validity of the 2-D model has been examined by comparing experimental and calculated results of the relationship between applied voltage and current of a primary transfer process in a printer. A schematic illustration of the primary transfer process is shown in Figure 4, and the field dependence of the electrical conductivity of the ITB is shown in Figure 5.

Shown in Figure 6 are experimental and calculated results with various charging potential on the OPC (Vd) on condition that toner is not developed. The good agreement supports the validity of the present model.

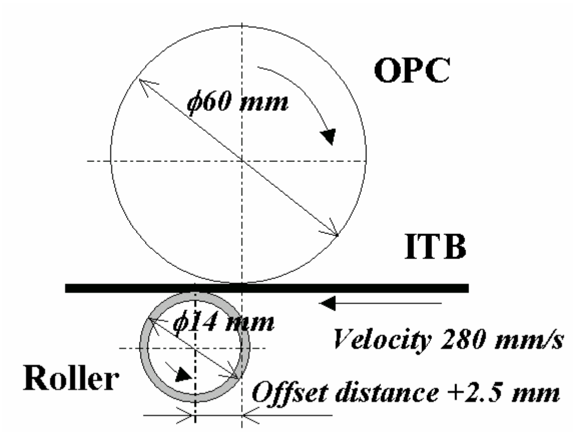

Figure 4. *A schematic illustration of the primary transfer process.*

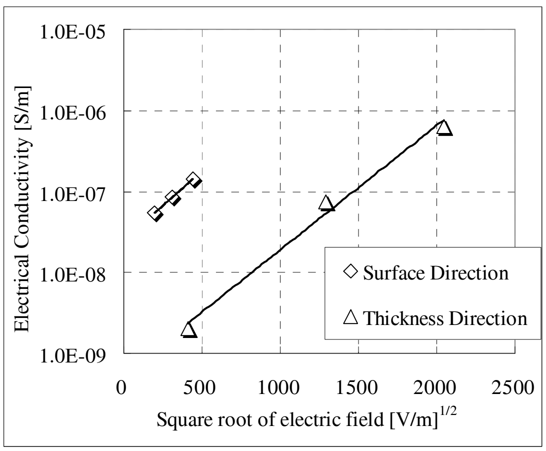

Figure 5. *The electric field dependence of the electrical conductivity of an intermediate transfer belt.*

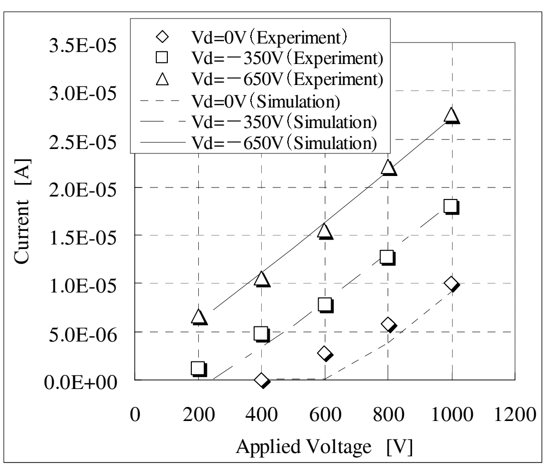

Figure 6. *A relationship between applied voltage and current of the primary transfer process.*

On the other hand, the validity of the 3-D model has been examined with a simple model experiment, where applied voltage dependence of transfer efficiency has been studied. A schematic illustration of the model experiment is shown in Figure 7. Developed toner on a PET-coated metal plate is approached to an opposite metal plate until contact is established and then is released, while a constant voltage difference is applied between the metal plates.

Figure 8 shows experimental and calculated results of the applied voltage dependence of transfer efficiency, and Figure 9 shows snapshots of the simulation at 1000 V. In the simulation, the averages of non-electrostatic forces of toner-OPC and toner-toner have been set to be 15 nN and 5 nN, respectively.

The transfer efficiency in the experiment increases with applied voltage up to about 900 V, and then decreases with applied voltage because the polarity of a part of toner charges is reversed by electrostatic discharge at a high applied voltage. The simulation result shows good agreement with the experiment, which supports the validity of the 3-D model.

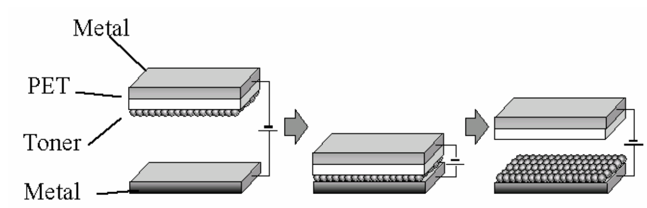

Figure 7. *A schematic illustration of the model experiment.*

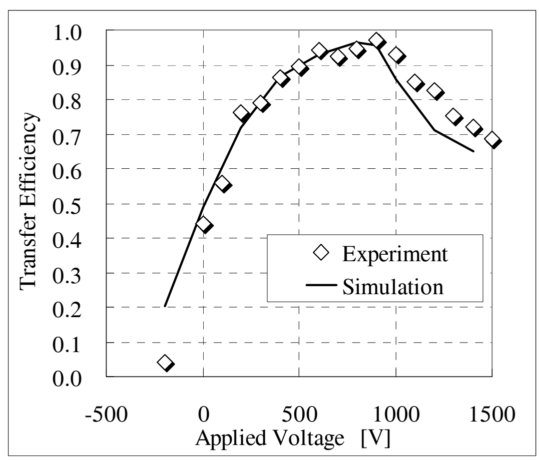

Figure 8. *The applied voltage dependence of transfer efficiency in the model experiment.*

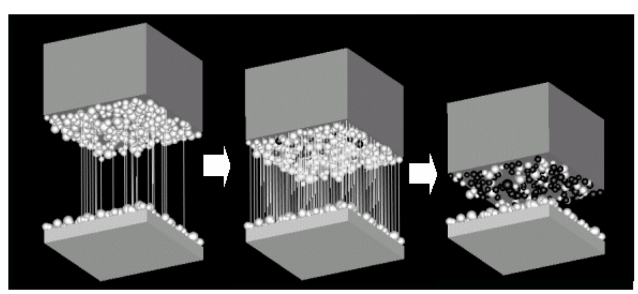

Figure 9. *Snapshots of the 3-D simulation. White and black particles are toner particles, which have negative and positive charges, respectively, and white lines in the transfer gap express electrostatic discharge.*

Simulation of Printer Process

Finally, analyses of a primary transfer processes in printers are demonstrated using the 2-D and the 3-D models. Figure 10 shows experimental and calculated results of the applied voltage dependence of transfer efficiency in the transfer process, shown in Figure 4. The results obtained by the simulation show good agreement with the experiments, and this suggests that transfer efficiency in printers is predictable by the analysis models.

On the other hand, shown in Figure 11 are one-dot images simulated with various offset distance between the primary transfer roller and the OPC in the direction of the ITB motion. In the results, toner scattering is increased by arranging the primary transfer roller in the upstream region, and the tendency can be observed in actual printers. This is because if the primary transfer roller is arranged in the upstream region, potential difference between the OPC and the ITB becomes large, as shown in Figure 12, and toner particles begin to move in the pre-nip area. The results suggest that a faithful transfer is accomplished by arranging a primary transfer roller in the downstream region.

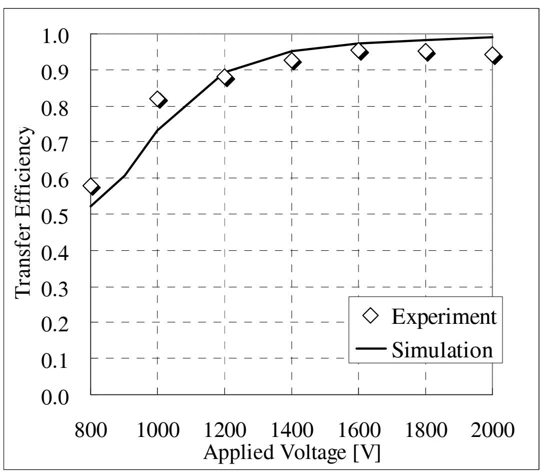

Figure 10. A relationship between applied voltage and transfer efficiency of the primary transfer process.

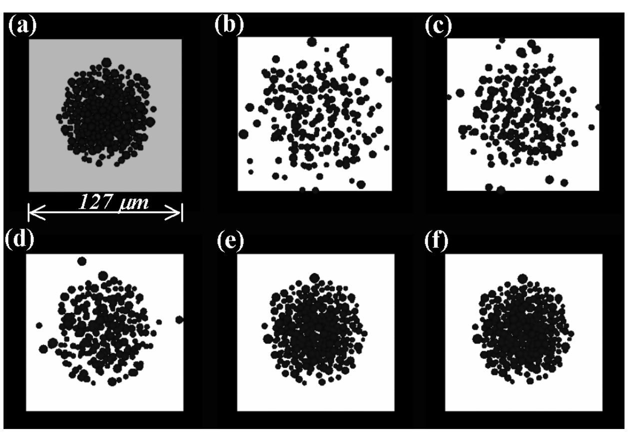

Figure 11. One-dot images obtained by the simulation. (a) is the developed image, and (b) to (f) are the transferred images on the ITB, which are obtained by offset distance of -2 mm, -1 mm, 0 mm, 1 mm, and 2 mm, respectively, on condition that applied voltage is 2000 V.

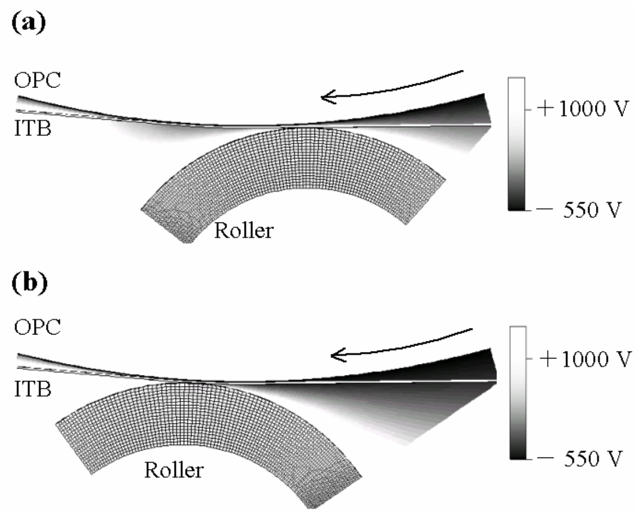

Figure 12. Potential distribution around transfer nips obtained by the 2-D simulation on condition that applied voltage is 2000 V. Offset distance of (a) is -2 mm and of (b) is 2 mm. White area, except for the ITB, shows where the electric potential is higher than 1000 V.

Conclusion

A simulation method using 2-D and 3-D models has been developed for analysis of primary transfer processes. By using the method, transfer efficiency and toner scattering can be predicted with a low computational load.

References

[1] Mark C. Zaretsky, "Performance of an Electrically Biased Transfer Roller in a Kodak ColorEdge CD Copier", J. Imaging. Sci. and Technol., 37, 2, pg. 187 (1993).
[2] N. Nakayama and H. Mukai, "Numerical Simulation of Electrostatic Transfer Process Using Discrete Element Method", Proc. Pan-Pacific Imaging Conference / Japan Hardcopy '98, pg. 261 (1998).
[3] Masami Kadonaga, "2-Dimensional Electrical Simulation of Intermediate Belt Transfer System", Proc. Japan Hardcopy 2001, pg. 293 (2001) [in Japanese].
[4] Toyoshige Sasaki, Seishirou Nasu, Tooru Nakaegawa, Makoto Saito and Jun Asai, "2-Dimensional Transfer Process Simulation Considering Toner Behavior", Proc. Japan Hardcopy 2004, pg. 287 (2004) [in Japanese].
[5] Masami Kadonaga, Tomoko Takahashi and Haruo Iimura, "Numerical Simulation of Toner Movement in a Transfer Process", Proc. NIP21, pg. 594 (2005).
[6] J. Frenkel, "On Pre-Breakdown Phenomena in Insulators and Electronic Semi-Conductors", Phys. Rev., 54, 8, pg. 647 (1938).
[7] R. M. Schaffert, Electrography (Focal Press, London, 1975) pg. 522.

Author Biography

Shinji Aoki received his M. Eng. in applied chemistry from Osaka Univ. in 1999. From 1999 to 2003 he worked for Toshiba Tec as a research engineer. He joined Ricoh in 2003 and has been engaged in R&D of electrophotography. He is a member of IS&T and ISJ.